9

Dynamics of the solar tachocline

PASCALE GARAUD

Department of Applied Mathematics and Theoretical Physics
University of Cambridge, Cambridge CB3 9EW, UK

Douglas Gough & Michael McIntyre proposed, in 1998, the first global and self-consistent model of the solar tachocline. Their model is however far more complex than analytical methods can deal with. In order to validate their work and show how well it can indeed represent the tachocline dynamics, I report on progress in the construction of a fully nonlinear numerical model of the tachocline based on their idea. Two separate and complementary approaches of this study are presented: the study of shear propagation into a rotating stratified radiative zone, and the study of the nonlinear interaction between shear and large-scale magnetic fields in an incompressible, rotating sphere. The combination of these two approaches provides good insight into the dynamics of the tachocline.

9.1 Introduction

The tachocline was discovered in 1989 by Brown et al.; it is a thin shear layer located at the interface of the uniformly rotating radiative zone and differentially rotating convective zone of the sun. Several issues about these observations remain unclear. Why is the radiative zone rotating uniformly despite the latitudinal shear imposed by the convection zone, and why is the tachocline so thin? How can the tachocline operate the dynamical transition between the magnetically spun-down convection zone and the interior? The first model of the tachocline was presented by Spiegel & Zahn (1992). They studied the propagation of the convection zone shear into the radiative zone under various hypotheses; in particular, they showed that in the case where angular momentum in the tachocline was transported only by isotropic viscosity the convection zone shear would propagate deep into the radiative zone within a local Eddington-Sweet timescale (rather than a viscous timescale) contrary to what is suggested by observations (Schou et al., 1998). Very roughly, the mechanism for shear propagation into a stratified region is the following: the existence of shear leads to a slight imbalance in the hydrostatic equilibrium and thereby drives meridional flows; these can burrow into the radiative zone, transporting and redistributing angular momentum deeper and deeper. Spiegel & Zahn then studied ways of confining the shear to a thin tachocline through angular-momentum transport by *anisotropic* Reynolds stresses; however, in a first part of this paper I would like to look a little more in detail at the isotropic case, as it can both be used in further investigations of the Gough & McIntyre model, as well as in more general studies of stellar rotation and rotational mixing.

9.2 One half of the problem: shear propagation into a rotating stratified fluid

In this first part, I will consider solar-type stars only and assume that their radiative zone is a stable, isotropic fluid with uniform viscosity μ_v, and that it has little influence on the dynamics of overlying convection zone. As a result, I will simply assume that the convection zone is imposing a given shear to the underlying stably stratified region. Also, I will assume that the dynamical timescale of this system is short compared to the stellar evolution timescale and the stellar spin-down timescale, so that I can limit my study to the steady-state case. This assumption will be dropped in future works on this subject. The equations describing this steady system are

$$
\begin{aligned}
&\rho_\mathrm{h}\boldsymbol{u}\cdot\nabla\boldsymbol{u} = -\nabla\tilde{p} - \rho_\mathrm{h}\nabla\tilde{\Phi} - \tilde{\rho}\nabla\Phi_\mathrm{h} + \mu_\mathrm{v}\nabla^2\boldsymbol{u} + \frac{1}{3}\mu_\mathrm{v}\nabla(\nabla\cdot\boldsymbol{u}) \ , \\
&\rho_\mathrm{h}T_\mathrm{h}\boldsymbol{u}\cdot\nabla s_\mathrm{h} = \nabla\cdot(k\nabla\tilde{T}) \ , \\
&\frac{\tilde{p}}{p_\mathrm{h}} = \frac{\tilde{\rho}}{\rho_\mathrm{h}} + \frac{\tilde{T}}{T_\mathrm{h}} \ , \\
&\nabla^2\tilde{\Phi} = 4\pi G\tilde{\rho} \ , \\
&\nabla\cdot(\rho_\mathrm{h}\boldsymbol{u}) = 0 \ ,
\end{aligned}
\qquad (9.1)
$$

where ρ, p and T are respectively the total density, pressure and temperature, $\boldsymbol{u} = (u_r, u_\theta, u_\phi \equiv r\ \sin\theta\,\tilde{\Omega})$ is the velocity field with respect to spherical polar coordinates (r, θ, ϕ), Φ is the gravitational potential, and k is the thermal conductivity. These equations are the first-order perturbation around the non-rotating hydrostatic background equilibrium (denoted by suffix h); this is a good approximation, as we will see, provided the centrifugal force is much smaller than the gravitational force. The background quantities $\rho_\mathrm{h}, p_\mathrm{h}, \Phi_\mathrm{h}$ and T_h are extracted from the standard solar model calculated by

Christensen-Dalsgaard et al. (1991). The perturbed quantities are denoted by tildes, $\tilde{p}, \tilde{\Phi}, \tilde{\rho}$ and $\tilde{T}$. The full nonlinearity of the momentum advection process is kept.

The boundary conditions used on the system are the following: the convection zone shear (as it is observed in the sun) is imposed at the top boundary and continuity of the stresses across the radiative-convective interface imposes another two conditions (on the continuity of the radial derivatives of the azimuthal and latitudinal velocities). A small impermeable core is removed from the region of computation near the centre to avoid singularities. This core is assumed to be rotating solidly, with a rotation rate $\Omega_{\rm in}$ determined through the steady-state condition that the total flux of angular momentum through the boundary is null. The regions outside the domain of simulation are assumed to be highly conductive so that they satisfy $\nabla^2 \tilde{T} = 0$, which provides the thermal boundary conditions to apply to the system.

Using the assumption of axisymmetry, I reduce the momentum equation in (9.1) to:

$$\boldsymbol{u} \cdot \nabla_\xi \left(\xi \, \sin\theta \, u_\phi\right) = \frac{E_\mu}{\rho_{\rm h}} {\rm D}^2 \left(\xi \, \sin\theta \, u_\phi\right) \ , \tag{9.2}$$

$$-\frac{1}{\rho_{\rm h}} \frac{\partial}{\partial z} \left(\rho_{\rm h} u_\phi^2\right) = -\frac{\sin\theta}{\rho_{\rm h}} \left(\frac{\partial \rho_{\rm h}}{\partial \xi} \frac{\partial \tilde{\Phi}}{\partial \theta} - \frac{1}{\epsilon} \frac{\partial \tilde{\rho}}{\partial \theta} \right) + \frac{E_\mu}{\rho_{\rm h}} {\rm D}^2 \left(\xi \, \sin\theta \, \omega_\phi\right) \ ,$$

where $\xi = r/r_{\rm c}$ is the new radial coordinate normalized by the radius $r_{\rm c}$ of the star, z is the normalized cylindrical coordinate that runs along the rotation axis, θ is the co-latitude, $E_\mu = \mu_{\rm v}/r_{\rm c}^2 \Omega_{\rm c}$ is the Ekman number, $\epsilon = r_{\rm c}^2 \Omega_{\rm c}^2 ({\rm l}\Phi_{\rm h}/{\rm l}\xi)^{-1}$ is the ratio of the centrifugal to gravitational forces, and $\omega = \nabla \times \boldsymbol{u}$ is the vorticity. In this expression the following normalizations have been applied: $[r] = r_{\rm c}$, $[u] = r_{\rm c}\Omega_{\rm c}$, $[\tilde{\Phi}] = r_{\rm c}^2 \Omega_{\rm c}^2$, $[T] = 1\,{\rm K}$, $[\rho] = 1\,{\rm g\,cm^{-3}}$, where $r_{\rm c}$ is the radius of the radiative zone and $\Omega_{\rm c}$ is the typical rotation rate of the star. The operator ${\rm D}^2$ is defined as

$${\rm D}^2 = \frac{\partial^2}{\partial \xi^2} + \frac{\sin\theta}{\xi^2} \frac{\partial}{\partial \theta} \left(\frac{1}{\sin\theta} \frac{\partial}{\partial \theta} \right) \tag{9.3}$$

The energy equation becomes, to first order in the thermodynamical perturbations

$$\epsilon T_{\rm h} \frac{\sigma N_{\rm h}^2}{\Omega_{\rm c}^2} \frac{\rho_{\rm h}}{E_\mu} u_r = \nabla_\xi^2 \tilde{T} \tag{9.4}$$

where σ is the Prandtl number, $N_{\rm h}$ is the background buoyancy frequency.

Finally, the equation of state can be combined with the radial and latitudinal components of the momentum equation to provide an expression for

$\tilde{\rho}$:

$$\frac{1}{\rho_{\rm h}}\frac{\partial\tilde{\rho}}{\partial\theta} = \frac{\rho_{\rm h}}{p_{\rm h}} r_{\rm c}^2\Omega_{\rm c}^2 \left[\frac{\cos\theta}{\sin\theta}u_\phi^2 - \frac{\partial\tilde{\Phi}}{\partial\theta}\right] - \frac{1}{T_{\rm h}}\frac{\partial\tilde{T}}{\partial\theta} \ . \tag{9.5}$$

Two standard approximations are often performed. The first one is the Boussinesq approximation, commonly used in studies of the tachocline, which is only justified when the thickness of the layer studied is much smaller than the background density scale-height. The second approximation consists in neglecting the effects of the mean centrifugal force on the system by supposing that its main contribution is a very small (negligible) oblateness of the hydrostatic background.

At the time of the Mons conference I presented numerical and analytical solutions of this system of equations and boundary conditions under both approximations. It has since appeared that both approximations were highly unjustified in this problem (as the bulk of the radiative zone spans many scale-heights, and as the mean centrifugal force creates a global baroclinicity of the system that must be taken into account) and lead to erroneous results. I now present instead the solution to the complete problem, solving the equations presented in (9.1). These equations are solved numerically, and the results suggest a scaling of the unknowns $\tilde{T}, u_r$ and u_θ which depends essentially on the parameter

$$\lambda = \sigma N_{\rm h}^2/\Omega_{\rm c}^2 \ . \tag{9.6}$$

9.2.1 Slow rotating case ($\lambda \gg 1$)

In the case of slow rotation, I find by studying the numerical results that $\tilde{T}$ and the poloidal components of the velocity $u_{r,\theta}$ scale the following way:

$$\begin{aligned} \tilde{T} &= \epsilon T_{\rm h}\overline{T} \ , \\ u_{r,\theta} &= E_\mu/(\lambda\rho_{\rm h})\overline{u}_{r,\theta} \ , \end{aligned} \tag{9.7}$$

where the quantities with bars are the scaled quantities, of order of unity. It is also found that $\tilde{\Phi}$ is always of order of unity, which is expected. Note that the scaling for the meridional motions is a local Eddington-Sweet scaling (see Spiegel & Zahn, 1992). Applying this ansatz to the system of equations given in (9.1), an expansion in powers of $1/\lambda$ reveals that the angular-momentum balance is dominated to zeroth order by viscous transport; thus

$$\mathrm{D}^2(\xi \ \sin\theta u_\phi) = 0 \ , \tag{9.8}$$

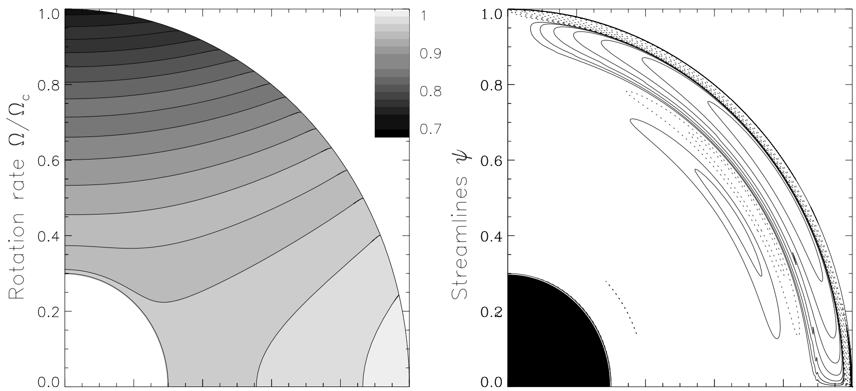

Fig. 9.1. Numerical solution of the system (9.1) for a solar-type star rotating 100 times slower than the sun ($\lambda \simeq 10^4$). The quadrants show the radiative zone only and the imposed shear at the top of the radiative zone is solar-like (i.e. $\tilde{\Omega}_{\rm cz} = (1 - 0.15\,\cos^2\theta - 0.15\,\cos^4\theta)$. The left panel shows the angular velocity, which is viscously dominated. The interior rotation rate is 0.957 times that imposed at the surface at the equator. The right panel shows the streamlines (dotted lines represent a clockwise flow, and solid lines represent an anti-clockwise flow). The contours are logarithmically spaced. The structure is reminiscent of Holton layers.

which determines the angular velocity profile uniquely. Using this result in the first order equations provides a relation between the temperature and gravitational potential perturbations:

$$\frac{p_{\rm h}}{\rho_{\rm h}}\frac{\partial}{\partial z}\left(\frac{\rho_{\rm h}}{p_{\rm h}}u_\phi^2\right) = \sin\theta\left(\frac{\partial\overline{T}}{\partial\theta} - \frac{{\rm d}\ln T_{\rm h}}{{\rm d}\xi}\frac{\partial\tilde{\Phi}}{\partial\theta}\right) ,$$
$$\frac{\partial}{\partial\theta}\nabla_\xi^2\tilde{\Phi} = -\frac{4\pi G\rho_{\rm h}r_{\rm c}}{g_{\rm h}}\left[\frac{{\rm d}\ln p_{\rm h}}{{\rm d}\xi}\left(\frac{\cos\theta}{\sin\theta}u_\phi^2 - \frac{\partial\tilde{\Phi}}{\partial\theta}\right) + \frac{\partial\overline{T}}{\partial\theta}\right] , \quad (9.9)$$

which can be solved independently for $\overline{T}$ and $\tilde{\Phi}$. Finally, the temperature fluctuations lead to meridional motions through

$$\overline{u_r} \simeq \nabla_\xi^2\overline{T} . \quad (9.10)$$

Figure 9.1 shows the results of the numerical solutions for the angular velocity profile and the meridional motions corresponding to a slowly rotating solar-type star (for which $\lambda \simeq 10^4$).

9.2.2 Fast rotating case ($\lambda \ll 1$)

In the case of fast rotation it is found that the correct scaling is

$$\tilde{T} = \lambda \epsilon T_{\rm h} \overline{T} \ ,$$
$$u_{r,\theta} = E_\mu / \rho_{\rm h} \overline{u}_{r,\theta} \ . \tag{9.11}$$

This time, I perform an asymptotic expansion in the small parameter λ. In this limit the temperature fluctuations are strongly damped by the rapid heat diffusion (as $\lambda \ll 1$ is equivalent to the small Prandtl number limit) and the system reaches an equilibrium which is determined by the zeroth order equations:

$$\frac{p_{\rm h}}{\rho_{\rm h}} \frac{\partial}{\partial z} \left(\frac{\rho_{\rm h}}{p_{\rm h}} u_\phi^2 \right) = - \sin\theta \frac{{\rm d} \ln T_{\rm h}}{{\rm d}\xi} \frac{\partial \tilde{\Phi}}{\partial \theta} \ ,$$
$$\frac{\partial}{\partial \theta} \nabla_\xi^2 \Phi = 4\pi G \frac{\rho_{\rm h}^2}{p_{\rm h}} \left[\frac{\cos\theta}{\sin\theta} u_\phi^2 - \frac{\partial \tilde{\Phi}}{\partial \theta} \right] \ . \tag{9.12}$$

These equations can in principle be solved for u_ϕ^2 and $\tilde{\Phi}$ and provide, to the next order in λ, the meridional flow through the advection diffusion balance:

$$\overline{\boldsymbol{u}} \cdot \nabla_\xi \left(\xi \ \sin\theta u_\phi \right) = {\rm D}^2 \left(\xi \ \sin\theta u_\phi \right) \ , \tag{9.13}$$

and, finally, the temperature fluctuations through

$$\overline{u} = \nabla_\xi^2 \overline{T} \ . \tag{9.14}$$

The results of the numerical simulations for small lambda ($\lambda \simeq 10^{-2}$) are shown in Fig. 9.2.

9.2.3 Solar rotation rate

In the solar case, the parameter λ varies between 0.1 and 1 in the region between the two boundaries. Although the solution is closer to the fast rotating case, the asymptotic analysis does not apply and the dynamics of the system result from a complex interaction of the momentum balance, the thermal energy advection-diffusion balance and the Poisson equation.

9.2.4 Discussion

I have studied the nonlinear dynamics of the radiative zone of a rotating solar-type star when a latitudinal shear is imposed by an overlying convection zone. This study is valid provided that the star is far from break-up (i.e. that the centrifugal force is small compared to the gravitational potential).

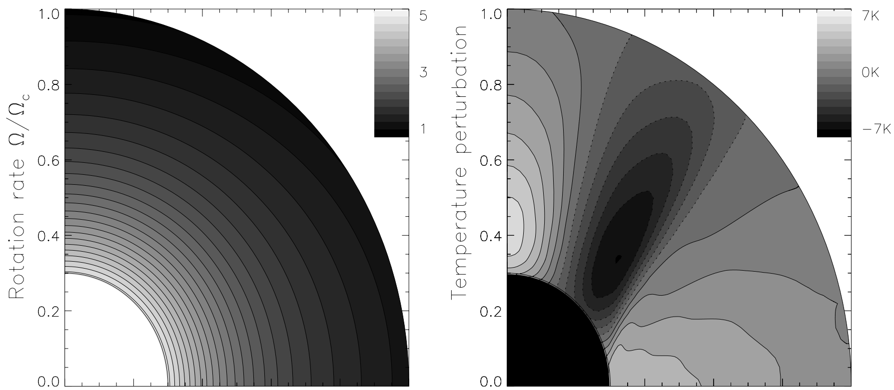

Fig. 9.2. Numerical solution of the system (9.1) for a solar-type star rotating 10 times faster than the sun ($\lambda \simeq 10^{-2}$). The left panel shows the angular velocity, which increases with depth through angular-momentum conservation. Note how the latitudinal variation of the angular velocity is small compared to its radial variation. The interior rotation rate is 5.26 times that imposed at the surface at the equator. The right panel shows the temperature fluctuations. Note that even when the stellar oblateness is of order of 10^{-3}, the temperature fluctuations remain of order of 10^{-6} through efficient heat diffusion.

I found that few approximations can be safely used in this study: the nonlinear advection terms and the effects of the centrifugal force must be carefully included in momentum equation. However, in the limit where the star is far from the break-up point, the perturbations to the hydrostatic background are found to be small indeed, which justifies the linearization of the equation of state.

Two asymptotic limits were found, which depend on the value of the parameter $\lambda = \sigma N_{\rm h}^2/\Omega_{\rm c}^2$. In the case of a slowly rotating star (with $\lambda \gg 1$) the hydrostatic background acquires a small ellipticity and the angular velocity profile is viscously dominated. The meridional flow velocities are of order of the local Eddington-Sweet velocity (e.g. Spiegel & Zahn, 1992) and take the shape of alterning dipolar cells reminiscent of the Holton layer structure. In the case of a fast rotating star (yet far from breakup), the temperature fluctuations are determined by an advection-diffusion balance which limits their amplitude to roughly $\lambda\epsilon T_{\rm h}$; this value is independent of the rotation rate. The angular velocity profile and the fluctuations in the gravitational potential can be determined independently through the momentum equation and the Poisson equation. It is found that the angular velocity increases sharply with depth, as expected from equation (9.2), and varies little with latitude. Similarly, the perturbation to the gravitational potential vary little with latitude, which suggests the possibility of approximating this limit analytically as a one-dimensional problem. This is under current investigation.

Finally, the effects of the boundary conditions on the problem (and in particular the presence of a lower rigid boundary) remain to be carefully analysed.

To summarize the first part of this paper, I have shown that it is possible to study semi-analytically (in some cases) and numerically the problem of shear propagation into the solar radiative zone in a self-consistent way, when taking into account isotropic viscosity only†. The main result is the following: as Spiegel & Zahn predicted, in this isotropic case the shear imposed by the convection zone penetrates all the way into the solar core. The failure to reproduce observations therefore suggests that other dynamical phenomena must be present in the solar radiative zone.

9.3 The other half of the problem: nonlinear interaction between a large-scale field and flows in a rotating sphere

Having studied the difficulty of hydrodynamical models to explain the structure of the solar tachocline, Gough & McIntyre (1998) suggested an alternative theory, namely that the observations could be reproduced through the existence of a large-scale fossil field in the solar radiative zone. As McGregor & Charbonneau (1999) showed, such a field can indeed impose a uniform rotation throughout most of the radiative zone and confine the shear to a thin tachocline provided none of the field lines are anchored into the convection zone‡: the field must be entirely confined to the radiative zone. Studies in the non-magnetic case following the lines described in the first part of this paper seem to suggest that shear-driven baroclinic imbalance leads to downwelling flows near the poles and the equator, with a localized upwelling in mid-latitudes (in regions of little shear). This phenomenon is illustrated in Fig. 9.3. Gough & McIntyre combined these two results and suggested that baroclinically driven flows could indeed lead to the confinement of the field through nonlinear advection, and proposed a new model of the tachocline based on this idea. However, only a fully nonlinear numerical study can verify whether this dynamical balance could indeed lead to the observed rotation profile.

As a first step towards a complete numerical simulation of the tachocline according to the Gough & McIntyre model, I have looked at the nonlinear

† Incidentally, it is clear that this type of analysis is not limited to the solar case, but can be applied to other stars with a wide range of rotation rates, masses, and ages. It will be interesting to compare the corresponding results to the asteroseismic observations of COROT.

‡ The shear would otherwise propagate along field lines according to Ferraro's isorotation law.

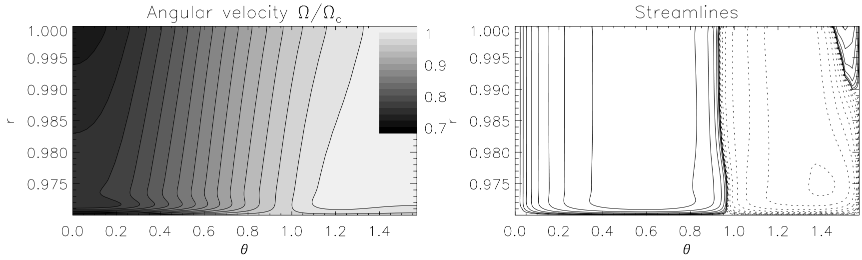

Fig. 9.3. Numerical solution of the system (9.1) for a solar-type star rotating with the observed solar angular velocity. The rigid bottom boundary was artificially placed at $r = 0.97r_{\rm c}$ to mimic the presence of a confined large-scale magnetic field. The left panel shows the angular velocity, when the convection zone shear is imposed at the top. The right panel shows the streamlines, with dotted lines representing clockwise flow and solid lines representing anti-clockwise flow. Note the two-cell structure with upwelling in mid-latitudes; note also the presence of an equatorial boundary layer.

interaction of a dipolar magnetic field and shear-driven motions only, when all thermal/compressibility effects are neglected. In these simulations, the fluid is incompressible with constant density ρ. This allows me to determine, through a simplified model, whether the idea of field confinement through meridional motions of the type described by Gough & McIntyre is indeed possible. In order to do this, I have created a numerical model in which meridional flows are created by the shear, not through baroclinic driving but through Ekman pumping on the boundary. The interest of this approach is that the geometry of the flow in this simplified problem is qualitatively similar to that shown in Fig. 9.3: it possesses a downwelling near the poles and the equator, and upwells in mid-latitude.

The numerical procedure is the following. I solve the following system of equations

$$\begin{aligned} 2(\hat{\boldsymbol{e}}_z \times \boldsymbol{u})_\phi &= \Lambda(\boldsymbol{j} \times \boldsymbol{B})_\phi + \frac{E_\mu}{\rho}(\nabla^2 \boldsymbol{u})_\phi \ , \\ [\nabla\times(\boldsymbol{u} \times \boldsymbol{B})]_\phi + E_\eta(\nabla^2 \boldsymbol{B})_\phi &= 0 \ , \\ \nabla\cdot\boldsymbol{u} &= 0 \ , \\ \nabla\cdot\boldsymbol{B} &= 0 \ , \end{aligned}$$

where $\boldsymbol{B}$ is the magnetic field, E_η is the magnetic Ekman number and Λ is the global Elsasser number defined as $\Lambda = B_0^2/\rho r_{\rm c}^2 \Omega_{\rm c}^2$. This system is solved in a spherical shell, where, as in the first part of this paper, the outer boundary corresponds to the bottom edge of the convection zone and the inner core is removed to avoid singularities. The outer boundary is now assumed to be impermeable in order to create artificially an Ekman layer at the interface with the convection zone which will drive the required meridional flows. A point dipole is placed at $r = 0$ such that the radial field at the pole at $r = r_{\rm in}$ is B_0. The regions outside the region of simulation are supposed to be conductive so that the magnetic field satisfies $\nabla^2 \boldsymbol{B} = 0$ in the steady state case. As in the first set of simulations, the inner core is rotating solidly with angular velocity $\Omega_{\rm in}$ where $\Omega_{\rm in}$ is determined through the steady-state requirement that the angular-momentum flux through the inner boundary is null.

The results are now discussed for fixed diffusive parameters, when only the Elsasser number is varied. For low Elsasser number ($\Lambda \ll 1$), the system is dominated by the Coriolis forces and the magnetic field is mostly passive. The shear imposed by the convection zone propagates deep into the radiative zone along the rotation axis, thereby satisfying Proudman's rotation law. Two meridional circulation cells are created by Ekman pumping on the outer boundary, with downwelling at the poles and the equator and upwelling in mid-latitudes, as required; they burrow deep into the radiative zone. In the limit of strong magnetic field (for $\Lambda \gg 1$) Lorentz forces rule the dynamics of the system; the poloidal field is barely affected by the rotation or the meridional motions and retain a dipolar structure throughout the interior. The shear propagates into the radiative zone along the field lines which have a footpoint in the convection zone, through Ferraro's isorotation theorem. Again this limit fails to reproduce the observations.

Only in the intermediate case ($\Lambda \simeq 1$) does the system begin to show the existence of a tachocline. Indeed, in this limit the field is still strong enough deep in the interior to dominate the dynamics of the system, but the meridional motions driven at the outer boundary manage to advect the field downwards near the equator thereby confining the field *into* the radiative zone in that region. At higher latitudes, however, some field lines retain their footpoints in the convection zone. As the field is mostly confined into the radiative zone, it imposes a state of near-uniform rotation save perhaps in a thin diffusive boundary layer near the top of the radiative zone and near the poles. This structure is reminiscent of the tachocline. Moreover, the meridional motions are confined to the shallower regions of the radiative zone by the underlying field; the consequences of the existence of this shallow mixing layer on the light element abundances is directly observable. The results of the simulations in the intermediate case are shown in Fig. 9.4.

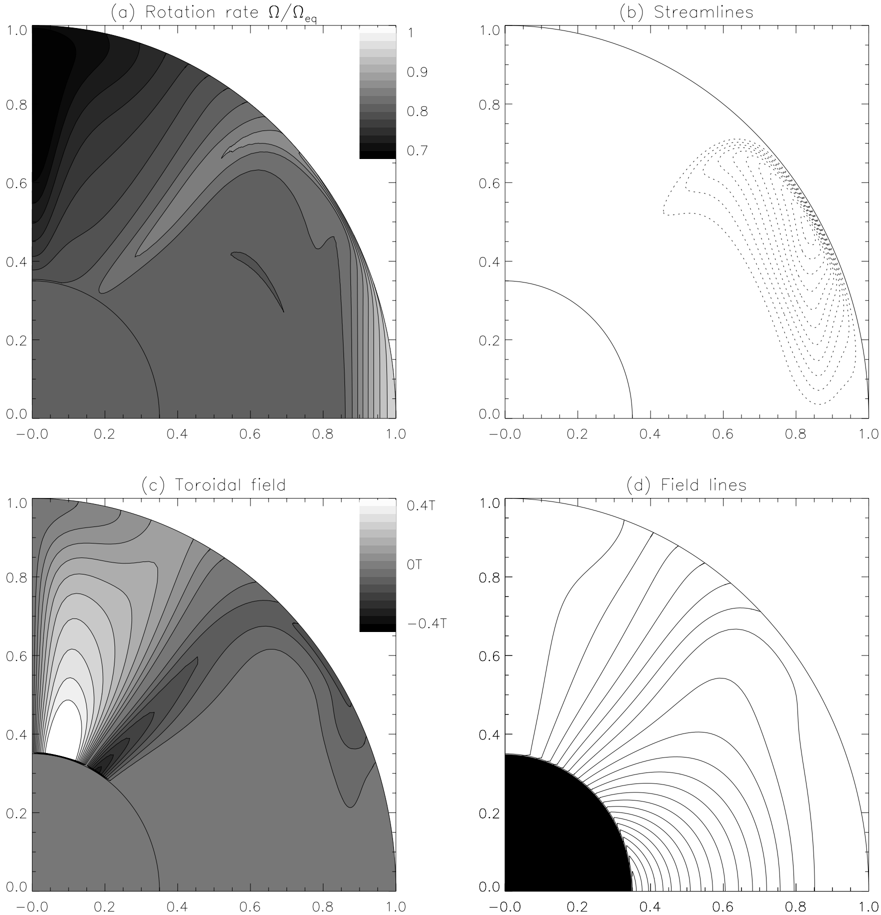

Fig. 9.4. Simulation results for $\Lambda = 1$, $E_\mu = 6.25 \times 10^{-5}$, and $E_\eta = 6.25 \times 10^{-5}$. Panel (a) shows the angular velocity, which is nearly uniform in the radiative zone whereas the shear is confined to the equatorial regions near the upper boundary, and around the poles. Panel (b) shows the meridional motions, which are confined to the upper layers of the radiative zone by the underlying magnetic field. The flow is downwelling at the equator and upwelling in mid-latitudes. Panel (c) shows the toroidal field, which is virtually null in regions of uniform rotation. Finally, panel (d) shows the poloidal field lines, which are confined in the radiative zone by the meridional motions.

9.4 Conclusion

It is now time to combine the results that we have learned from these two separate studies of the rotation profile in the radiative zone and relate them to the tachocline dynamics.

The model of the tachocline proposed by Gough & McIntyre (1998) attempts to solve the following problem: how can we explain that the solar radiative zone is rotating uniformly when a study of standard stellar rotation would normally suggest the existence of strong shear. Gough & McIntyre suggested that the interaction of a large-scale field and baroclinically driven meridional motions in the tachocline could lead to the observed angular velocity profile. This model hangs on two key points: the magnetic field must be entirely confined to the radiative zone to impose uniform rotation, and the meridional motions must be confined to the tachocline to explain both the required two-cell structure (which can then in turn confine the field) and the observed light element abundances (Elliott & Gough, 1999).

By studying the dynamics of a thin layer of stratified fluid representing the tachocline I have shown that baroclinic effects do indeed lead to a two-cell circulation with upwelling in mid-latitudes and downwelling near the poles and the equator. I have then taken a complementary approach and looked at the dynamical interaction between such a two-cell circulation and a dipolar large-scale field. This allowed me to show that the meridional motions can indeed confine this field to the radiative zone for some range of values of the magnetic field strength. The confined field imposes a uniform angular velocity to most of the radiative interior, save in a thin tachocline where all the dynamical interactions described above take place.

To conclude, I believe that these preliminary analyses show that the model proposed by Gough & McIntyre possesses the right physical elements for the description of the dynamics of the tachocline. There remains now only the task of completing this work through the numerical resolution of their whole model.

Acknowledgments I thank Douglas Gough for his help and his encouragements throughout my PhD thesis and in the year that has followed. This work has benefited immensely from his sharp and inspired vision of the subject.

References

Brown, T. M., Christensen-Dalsgaard, J., Dziembowski, W. A., Goode, P., Gough, D. O. & Morrow, C. A., 1989, *ApJ*, **343**, 526
Christensen-Dalsgaard, J., Gough, D. O. & Thompson, M. J., 1991, *ApJ*, **378**, 413
Elliot, J. R. & Gough, D. O., 1999, *ApJ*, **516**, 475
Gough, D. O. & McIntyre, M. E., 1998, *Nature*, **394**, 755
MacGregor, K.B. & Charbonneau, P., 1999, *ApJ*, **519**, 911
Schou, J. et al., 1998, *ApJ*, **505**, 390
Spiegel, E. A. & Zahn, J.-P., 1992, *A&A*, **265**, 106